Synthesis, Spectral Studies, and Microbial Activity of Mn (II), Ni (II), Cu (II), Zn (II), Pd (II), Pt (II) Complexes with Schiff Base Ligand

Pooja P Batawale, Manosha G Kapade, Uttra M Dalvi, Manohar V Lokhande*

Department of Chemistry, Sathaye College (Autonomous), Mumbai-400057, Maharashtra, India.

Abstract: Novel Schiff base metal ion complexes of Manganese (II), Nickel (II), Copper (II), Zinc (II), Platinum (II) and Palladium (II) were synthesised via a condensation reaction between 3-amino-1,4-benzodioxine -2-carbaldehyde , and 3-aminopyridin-2-ol yielding the ligand 3-{(*Z*)-[(3-amino-1,4-benzodioxin -2-yl) methylidene]amino}pyridin-2-ol The resulting complexes were characterised using various spectral techniques, including Fourier Transform Infrared (FTIR) spectroscopy, Ultraviolet-Visible (UV-Vis) spectroscopy, Thermogravimetric/Differential Thermal Analysis (TGA/DTA), and Mass Spectrometry. Conductance measurements, magnetic susceptibility, and metal content estimations were also performed to assess the physicochemical properties of the complexes.

The experimentally determined molecular mass of the Schiff base closely matched its theoretical value, confirming successful synthesis. Fourier Transform Infrared (FTIR) spectroscopy confirms the coordination of the ligand to the metal ions through the imino (>C=N), metal–oxygen (M–O), and metal–nitrogen (M–N) functional groups. Thermal analysis further verifies the presence of two coordinated water molecules attached to the metal center. Upon heating, these water molecules are eliminated, ultimately leading to the formation of the corresponding metal oxide. UV-Vis spectral analysis revealed that all complexes were coloured, except for the Zinc (II) complex, which appeared colourless. Parameters such as the nephelauxetic effect, covalence factor ($b^{1/2}$), and percentage covalency (δ%) were calculated, indicating that the complexes exhibit covalent character. The central metal ions possess a coordination number of eight, and the ligand acts as a bidentate donor. Finally, the antimicrobial activities of the synthesised Schiff base and its metal complexes were evaluated.

Keywords: Schiff base, Metal ions, FTIR, Ultraviolet−Visible, Mass, TGA/DTA

Introduction: Schiff base ligands have attracted considerable attention from researchers due to their diverse physicochemical properties and versatile structural frameworks [1-2]. These features have led to extensive exploration of their potential applications. Their structural flexibility allows Schiff bases to function effectively as asymmetric and stabilising agents for metal complexes across various oxidation states [3-4]. Moreover, Schiff bases play a pivotal role in modulating metal reactivity in numerous catalytic and transformation processes. The presence of nitrogen and oxygen donor atoms facilitates the formation of stable tetradentate complexes [5-6]. Notably, certain azo-

azomethine metal complexes exhibit promising photophysical properties and energy transfer capabilities, making them valuable in technological applications. Their thermochromic, photochromic, and electroactive properties, along with chemical stability [7-8], render Schiff base compounds suitable intermediates for a wide array of functional materials.

Comprehensive reviews have highlighted the significance of their metallo-organic chemistry, particularly in influencing biological activity and underscoring the catalytic role of metal centres in biochemical pathways [9]. The planarity of the >C=N– group, coupled with the bonding orbitals of electronegative atoms, enhances electron delocalisation and adsorption onto metal surfaces. These electronic attributes contribute to the efficacy of Schiff base metal complexes as corrosion inhibitors for mild steel [10-11]. Kargar and co-workers successfully synthesised tetradentate Schiff base ligands and their corresponding metal complexes using methoxy salicylaldehyde and substituted phenylenediamine [12]. Their findings revealed that these complexes exhibit notable catalytic efficiency. The growing relevance of Schiff base compounds can be attributed to the high reactivity and facile synthesis of the azomethine (>C=N–) functional group, typically formed via a temperature-regulated condensation reaction between a reactive carbonyl compound and a primary amine [13-14].

While antimicrobial agents have proven effective against bacterial infections, the escalating issue of antibiotic resistance necessitates the development of innovative molecular frameworks. Metal complexes, particularly those derived from Schiff base ligands, offer promising avenues due to their diverse activity profiles. These compounds have demonstrated significant potential across electrical, pharmacological, and biological applications[15].

Recent advancements in computational chemistry, molecular modelling, and docking techniques have accelerated the discovery of transition-metal-based systems. This progress has enhanced the efficiency of electronic structure-property screening, facilitating the rational design of functional metal complexes for targeted applications [16-17].

In this study, a new Schiff base ligand was synthesized from 3-amino-1,4-benzodioxine -2-carbaldehyde , and 3-aminopyridin-2-ol yielding the ligand 3-{(Z)-[(3-amino-1,4-benzodioxin -2-yl) methylidene]amino}pyridin-2-ol, followed by the formation of its metal complexes with Mn (II), Ni (II), Co (II), Cu (II), Zn (II), Pt (II) , and Pd(II) ions. The structural features of both the ligand, and its complexes were systematically characterised. Additionally, their antimicrobial efficacy was evaluated against selected bacterial and fungal strains.

Materials and Methods: The chemical compounds 3-amino-1,4-benzodioxine-2-carbaldehyde and 3-aminopyridin-2-ol were obtained from Sigma-Aldrich and used without further purification. Metal chlorides and nitrates were obtained from SD Fine Chemicals and used as received.

Synthesis of the Ligand: The ligand was synthesised by refluxing a 2:3 molar ratio of 3-amino-1,4-benzodioxine-2-carbaldehyde and 3-aminopyridin-2-ol in 40 mL of ethanol. A few drops of glacial acetic acid were added to facilitate the reaction, which was carried out under reflux using a water condenser for two hours. When the complete reaction a coloured precipitate was formed. The precipitate was subsequently filtered, washed thoroughly with ethanol, and dried in an oven at 55 °C.

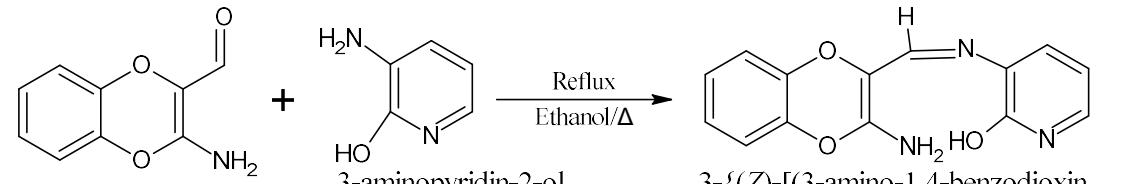

3-amino-1,4-benzodioxine -2-carbaldehyde + 3-aminopyridin-2-ol → 3-{(*Z*)-[(3-amino-1,4-benzodioxin -2-yl) methylidene]amino}pyridin-2-ol

Synthesis of Metal Complexes:

Schiff base metal complexes of Manganese(II), Cobalt(II), Nickel(II), Copper(II), Zinc(II), Platinum (II) and Palladium(II) were synthesised using metal-to-ligand (M : L) molar ratios of 2:1, 2:3, and 1:3. a) In a round-bottom flask, 60 cm^3 of Schiff base solution and 30 cm^3 of metal chloride or nitrate, b) In a round-bottom flask, 60 cm^3 of Schiff base solution and 40 cm^3 of metal chloride or nitrate, and c) In a round-bottom flask, 60 cm^3 of Schiff base solution and 20 cm^3 of metal chloride or nitrate, solution were combined and stirred vigorously on a hot plate with a magnetic stirrer. The reaction mixture was then refluxed for approximately four hours with the addition of a few drops of ethanol and aqueous ammonia to facilitate complexation. After refluxing, the solution was kept in a dark place overnight to allow the formation of solid complexes. The resulting precipitates were filtered and dried in a vacuum desiccator. Both the Schiff base ligand and its metal complexes were found to be soluble in dimethyl sulfoxide (DMSO) and dimethylformamide (DMF).

Results and Discussion:

The synthesised ligand exhibits a sharp melting point and distinct colouration, similar to its corresponding octahedral metal complexes. These complexes readily dissolve in solvents such as DMSO and DMF. The calculated analytical values support the proposed structural formulations. Metal content—Manganese (6.93%), Cobalt (7.39%), Nickel (7.37%), Copper (7.93%), Palladium (12.60%), Platinum (II), and Zinc (8.148%) was determined using volumetric techniques and atomic absorption spectroscopy (AAS), with AAS specifically employed for the quantification of Pt (II) and Pd (II). Molar conductance measurements in DMSO were performed using an Equi-Tronics digital conductivity meter. The magnetic properties of the complexes were evaluated and compared with established literature references [18-19], confirming their octahedral geometry. All complexes exhibit neutral ionic molar conductivity. Table 1 presents the molar conductance, magnetic moments, physical parameters, and relative coordination numbers (CN) for the complexes

MnL_2, NiL_2, CoL_2, CuL_2, PtL_2, PdL_2, and ZnL_2. The magnetic and conductivity data further substantiate the octahedral configuration of these metal-ligand systems.

Table -1: Analytical and Physical Data (* Experimental)

Complexes/Ligand	MP/DP°C	% Yield	C%	N%	M%	Conductivity	μ_{eff} BM
($C_{14}H_{11}N_3O_3$)	114-117	73%	62.45	15.61	-	-	-
			62.42*	15.58*	-		
[Mn($C_{28}H_{20}N_6O_6$)]	198-201	55%	56.86	14.21	9.29	4.31	5.14
			56.78*	14.17*	9.22*		
[Ni ($C_{28}H_{20}N_6O_6$)]	210-213	59%	56.50	14.12	9.86	4.45	3.15
			56.44*	14.08*	9.78*		
[Co($C_{28}H_{20}N_6O_6$)]	221-224	52%	56.48	14.11	9.90	4.59	4.52
			56.42*	14.05*	9.78*		
[Cu($C_{28}H_{20}N_6O_6$)]	217-220	65%	56.05	14.01	10.59	4.71	2.14
			55.98*	14.92*	10.47*		
[Zn($C_{28}H_{20}N_6O_6$)]	212-214	62%	55.87	13.96	10.87	4.83	Dimag
			55.77*	13.87*	10.79*		
[Pt($C_{28}H_{20}N_6O_6$)]	242-245	52%	45.97	11.49	26.67	4.92	-
			45.77*	11.31*	26.49*		
[Pd($C_{28}H_{20}N_6O_6$)]	251-254	55%	52.31	13.07	16.55	4.99	-
			52.18*	12.91*	16.38*		

Infrared Spectra of Schiff Base and Complexes : The infrared spectra of the ligand and the metal complexes were recorded. The infrared spectral bands of the free ligand and its metal complexes. The possible peaks of Schiff's base in FTIR are: Phenolic OH on pyridin-2-ol contributes to a broad hydrogen-bonded O–H stretch at 3420 cm^{-1}. The imine linkage (–CH=N–) [20] from Schiff base formation yields a strong >C=N- stretch at 1635 cm^{-1}. The primary amine on benzodioxin contributes -N–H stretches at 3244cm^{-1}. Aromatic rings from both benzodioxin and pyridine contribute characteristic >C–H and -C=C- vibrations at 1450cm^{-1}. Aromatic rings from both benzodioxin and pyridine contribute characteristic >C–H and -C=C- vibrations at 1475cm^{-1}. The ether bridge in benzodioxin shows up in the fingerprint region at 1190cm^{-1}.

The FTIR Spectra in the complexes are: The Phenolic –OH on pyridin-2-ol can deprotonate and coordinate via oxygen. Disappearance or shift of O–H (phenolic) stretching indicates deprotonation and coordination. Imine nitrogen (>CH=N–), strong donor to metal ions, and it's shifted to from 1635 to 1618cm^{-1}. Amino group (–NH_2) on benzodioxin, a potential donor depending on geometry and steric, is shifted to lower frequencies, ranging from 0-25cm^{-1}. Pyridine nitrogen excellent donor to transition metals and forms a complex. The two bands observed for (M-N) bond at 570-575 cm^{-1} ,and (M-O) bonds in the range 490-495 $cm^{-1,}$ respectively [21]. Two new broad bands for coordinated water molecules are seen in IR spectra at 3440 cm^{-1} and 3505 cm^{-1} [22].

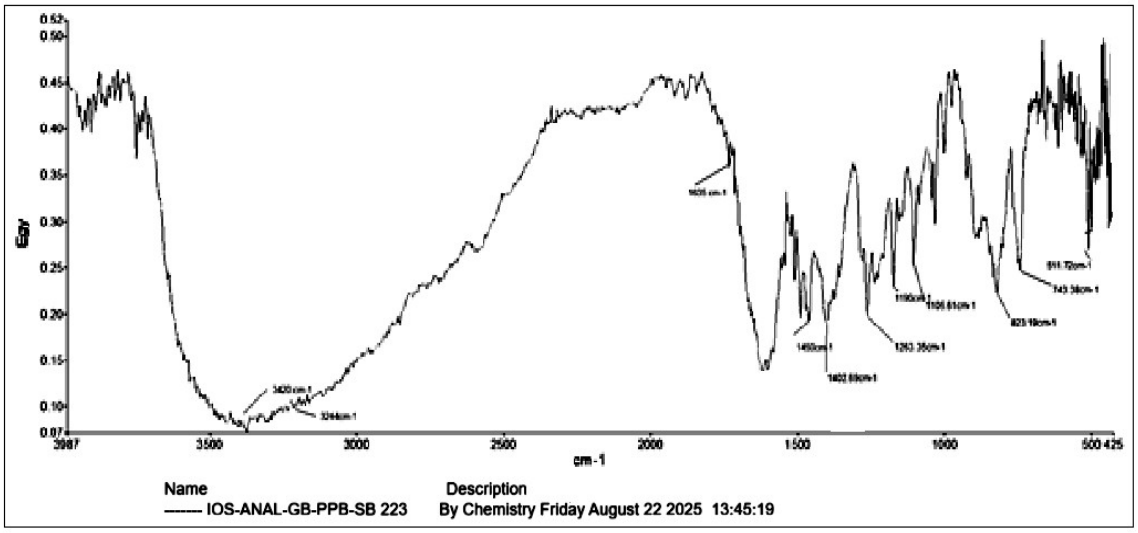

Figure 1: FTIR of Schiff Base

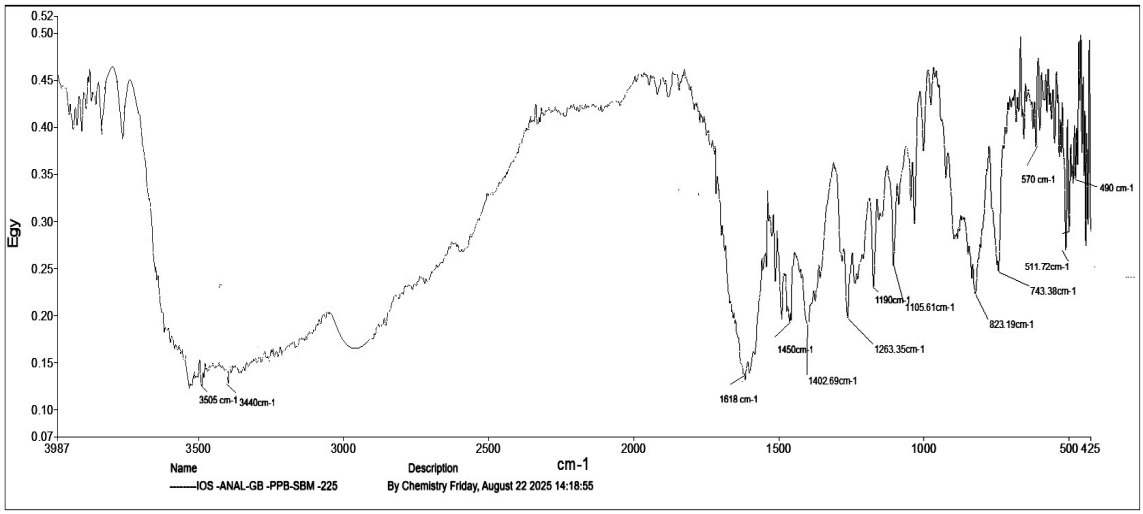

Figure 2: FTIR of Mn(II) Schiff Base ligand complex

Table 2: FTIR of Schiff base ligand and metal complexes (in cm^{-1})

L/Complexes	**vOH**	**vHC=N**	**vH_2O**	**vH_2O**	**vNH_2**	**vM-O**	**vM-N**
($C_{14}H_{11}N_3O_3$)	3440	1645	-	-	3255	-	-
[Mn($C_{28}H_{20}N_6O_6$)]	-	1618	3445	3490	3220	480	565
[Ni ($C_{28}H_{20}N_6O_6$)]	-	1620	3435	3510	3222	482	570
[Co($C_{28}H_{20}N_6O_6$)]	-	1624	3448	3502	3224	475	568
[Cu($C_{28}H_{20}N_6O_6$)]	-	1628	3452	3498	3220	472	565
[Zn($C_{28}H_{20}N_6O_6$)]	-	1625	3447	3594	3218	478	563

Magnetic Properties and Electronic Spectra of Transition Metal Complexes: The Bohr magneton (BM) serves as a fundamental unit for quantifying the magnetic field strength associated with an electron. The magnetic moment (\mu) of a transition metal ion is determined using the expression √n(n+2)} BM, where n denotes the number of unpaired electrons [23-24]. Ions possessing unpaired electrons exhibit paramagnetic, rendering them susceptible to external magnetic fields. Elements of the first transition series typically form vividly coloured ions and compounds due to their partially filled d-orbitals. Table 3 presents the magnetic moment values and

electronic spectral data for complexes of Mn (II), Co (II), Ni (II), and Cu (II). These measurements were conducted at room temperature in dimethyl sulfoxide (DMSO) at a concentration of 10^{-3} M [25-26].

Mn (II) Complex: The electronic spectrum revealed a single absorption band at 575 nm, attributed to the $^6A_{1g} \rightarrow {}^4T_{2g}(G)$ transition, indicative of an octahedral geometry. The observed magnetic moment of 5.15 BM corroborates this structural assignment.

Co (II) Complex: A prominent absorption band at 587 nm corresponds to the $^4T_{1g}(F) - {}^4A_{2g}(F)$ transition in an octahedral field. The magnetic moment of 4.38 BM suggests the presence of three unpaired electrons, consistent with an octahedral configuration.

Ni (II) Complex: The spectral profile exhibited three distinct bands at 445 nm, 520 nm, and 640 nm, associated with the transitions $^3A_{2g} \rightarrow {}^3T_{2g}$, $^3A_{2g}(F) \rightarrow {}^3T_{1g}(F)$, and $^3A_{2g}(F) \rightarrow {}^3T_{1g}(P)$, respectively. These transitions further affirm the octahedral stereochemistry of the Ni (II) complex. The magnetic moment value indicates the octahedral geometry surrounding the Ni (II) ion, which is 3.18 B.M [28].

Cu (II) Complex: The electronic absorption spectrum of the Cu (II) complex displays two distinct bands at 610 nm and 650 nm, which correspond to the $^2B^{1g} - {}^2Eg$ and $^2B_{1g} - {}^2B_{2g}$ transitions, respectively. A magnetic moment of 2.04 Bohr Magnetons (B.M.) suggests the presence of a single unpaired electron within an octahedral coordination environment. In contrast, Zn (II) complexes are diamagnetic due to the absence of unpaired electrons and typically form colourless solutions, reflecting their filled d-orbital configuration.

Table 3 : Electronic Spectra and Their Parameter

Complexes	Bands (nm)	β	1-β	$\beta^{1/2}$	η	$b^{1/2}$	δ%
$[Mn(C_{28}H_{20}N_6O_6)]$	515	0.9665	0.0335	0.9831	0.0172	0.09151	1.7485
$[Ni\ (C_{28}H_{20}N_6O_6)]$	402,480,645	0.9740	0.0260	0.9869	0.0133	0.08061	1.3449
$[Co(C_{28}H_{20}N_6O_6)]$	422,620	0.9675	0.0325	0.9836	0.0168	0.09014	1.6950
$[Cu(C_{28}H_{20}N_6O_6)]$	610,650	0.9745	0.0255	0.9871	0.0131	0.07984	1.3237

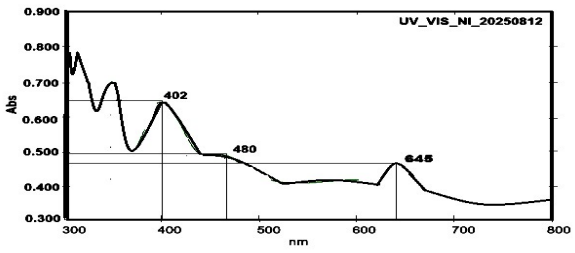

Figure 3: UV-VIS of Ni(II) Complex

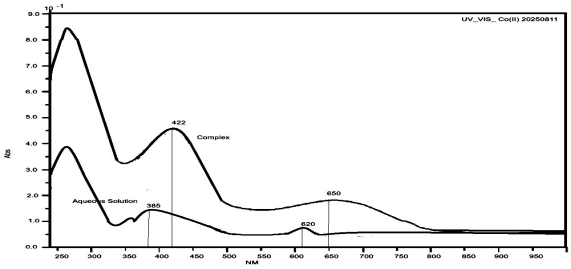

Figure 4: UV-VIS of Co(II) Complex

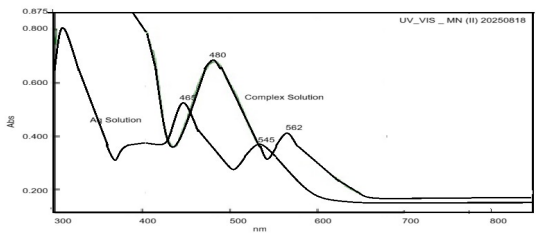

Figure 5: UV-VIS of Mn (II) Complex

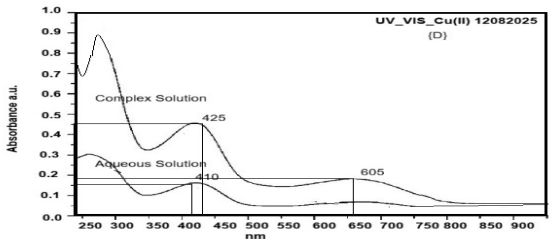

Figure 6: UV-VIS of Cu(II) Complex

Thermal analysis: Thermogravimetric (TGA) and differential thermal analysis (DTA) data for the complexes $[Co(C_{28}H_{20}N_6O_6)]$,$[Pd(C_{28}H_{20}N_6O_6)]$ indicate that both compounds exhibit thermal stability at ambient conditions and undergo multi-step decomposition. The observed mass losses correspond to both endothermic and exothermic transitions [27].

$[Co(C_{28}H_{20}N_6O_6)]$ complex:

- The initial weight loss, occurring between 50°C and 205°C, is attributed to the release of two coordinated water molecules along with partial degradation of the chelate structure. The experimental mass loss recorded is 11.15% (10.85%), which aligns closely with the theoretical prediction. This phase is marked by an endothermic peak in the DTA curve
- The decomposition is observed between 270°C and 325°C, with a corresponding experimental weight loss of 18.14 % (17.94%), again consistent with theoretical values. An exothermic peak in the DTA profile characterises this stage
- A major decomposition is observed between 330°C and 475°C, with a corresponding experimental weight loss of 19.22 % (19.01%), again consistent with theoretical values
- At elevated temperatures ranging from 500°C to 900°C, the residue primarily consists of the corresponding Cobalt (II) oxide

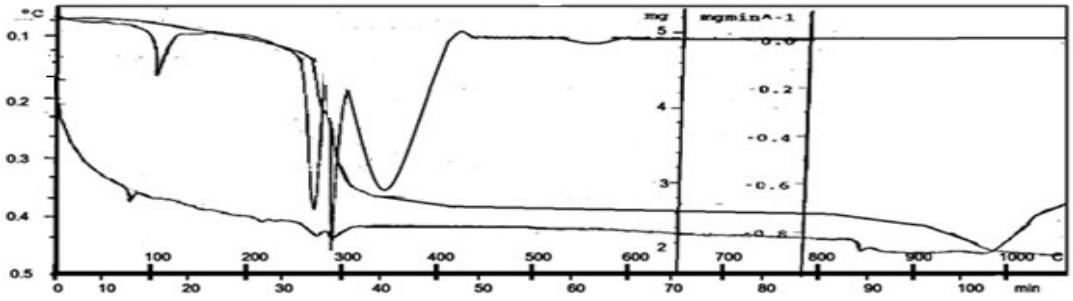

Figure 7: TGA/DTA of $[Co(C_{28}H_{20}N_6O_6).2H_2O]$ Complex

- Thermal analysis of the Pt^{2+} complex reveals a four-step decomposition profile. The initial phase, occurring between 50°C and 250°C, involves the release of two coordinated water molecules along with partial degradation of the complex. The thermogravimetric curve indicates a mass loss of 15.78% (15.50%), which closely matches the theoretical estimate. This stage is marked by an endothermic peak in the differential thermal analysis
- The second decomposition step takes place between 255°C and 380°C, where fragments such as C_6H_4N are likely eliminated. This phase is characterised by an exothermic peak in the DTA curve, suggesting significant structural breakdown
- In the third stage, spanning 400°C to 550°C, a substantial portion of the chelating ligand is lost. The observed weight reduction is 21.12%, aligning well with the calculated value of 20.88%.
- Finally, in the temperature range of 560°C to 850°C, the residual material undergoes further transformation, resulting in the formation of palladium m oxide.

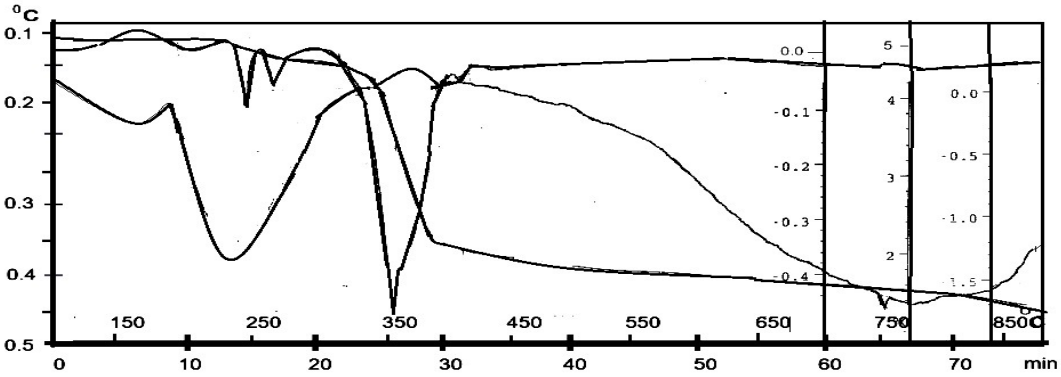

Figure 8: TGA/DTA of [Pd($C_{28}H_{20}N_6O_6$).2H_2O] Complex

Mass Spectra of Schiff Base and Complexes: Mass spectrometric analysis of the ligands and their corresponding metal complexes, recorded at ambient temperature, is summarised in the table below. The calculated mass of the Schiff base is m/z =269.255, and the found mass is m/z = 269.245. The calculated molecular ion peak for the Mn (II) complex is m/z = 627.47, while that of the Zn (II) complex is m/z = 637.91. However, the observed peaks appear at m/z = 627.4 and 637.91, respectively, indicating the presence of [M+1] species. These peaks affirm the proposed molecular structures of the complexes. The appearance of multiple ion fragments in the spectra is attributed to the stepwise fragmentation of the metal complex molecules, resulting from cleavage of internal bonds and subsequent formation of various radical species, which give rise to additional prominent peaks.

Table-4: Mass spectra of the Schiff bases and complexes

Ligand/Complex	Expected m/z	Found m/z	Peak assigned
($C_{14}H_{11}N_3O_3$)	269.25	269.24	M
[Mn($C_{28}H_{20}N_6O_6$).2H_2O]	627.47	627.43	M+1
[Ni ($C_{28}H_{20}N_6O_6$).2H_2O]	631.23	631.21	M
[Co($C_{28}H_{20}N_6O_6$).2H_2O]	631.46	631.43	M
[Cu($C_{28}H_{20}N_6O_6$).2H_2O]	636.08	637.04	M
[Zn($C_{28}H_{20}N_6O_6$).2H_2O]	637.91	638.90	M+1
[Pt ($C_{28}H_{20}N_6O_6$).2H_2O]	749.59	-	M
[Pd($C_{28}H_{20}N_6O_6$).2H_2O]	660.93	-	M

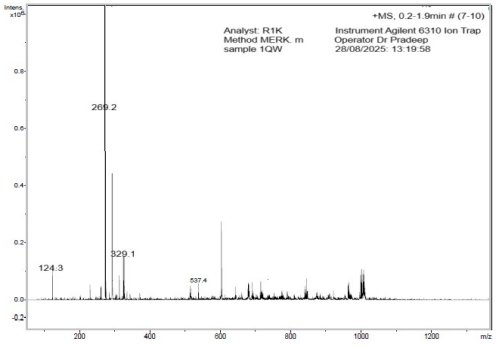

Figure 9: Mass of Schiff Base

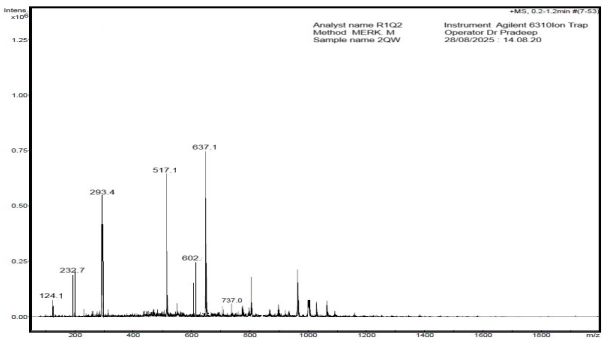

Figure 10: Mass spectra of Zn(II) Complex

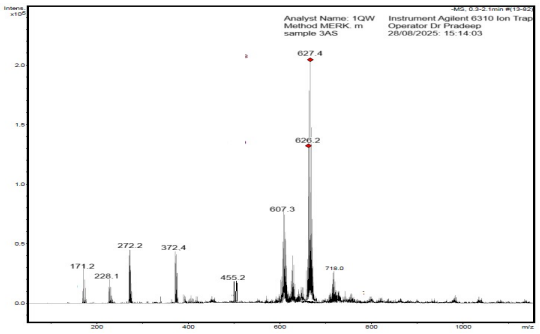

Figure 11: Mass spectra of Mn(II) Complex

Microbial activity: The antibacterial efficacy of the synthesised Schiff base and its metal (II) complexes was evaluated in vitro using the agar gel diffusion technique. The compounds were tested against two Gram-positive bacterial strains, *Bacillus subtilis* and *Staphylococcus aureus,* as well as two Gram-negative strains, *Shigella flexneri* and *Pseudomonas aeruginosa[00]*. Petri dishes were incubated at 37°C for 24 hours immediately after inoculation. Antimicrobial activity was assessed by measuring the diameter (in mm) of the inhibition zones. Comparative analysis was performed against standard antibiotics to determine relative potency. Control experiments using DMSO alone confirmed that the solvent exhibited no inhibitory effect on any of the tested bacterial strains. All results were expressed as inhibition zone diameters and benchmarked against reference drugs[28-30]

Table 5: Microbial activity of Schiff Base and Complexes

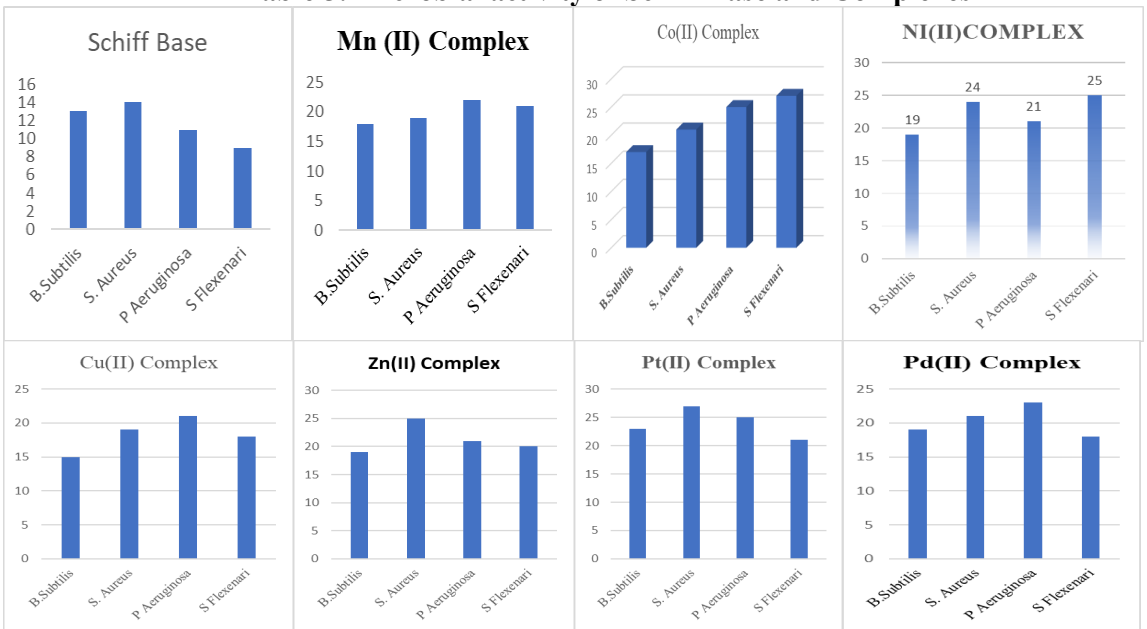

	B Subtilis	S Aureus	S Flexenari	P Aeruginosa
($C_{14}H_{11}N_3O_3$)	13	14	10	09
[Mn ($C_{28}H_{20}N_6O_6$).$2H_2O$]	17	19	21	20
[Ni ($C_{28}H_{20}N_6O_6$).$2H_2O$]	19	24	21	25
[Co ($C_{28}H_{20}N_6O_6$).$2H_2O$]	15	20	24	25
[Cu ($C_{28}H_{20}N_6O_6$).$2H_2O$]	15	19	21	18
[Zn ($C_{28}H_{20}N_6O_6$).$2H_2O$]	19	25	21	20

[Pt ($C_{28}H_{20}N_6O_6$).$2H_2O$]	23	27	25	21
[Pd ($C_{28}H_{20}N_6O_6$).$2H_2O$]	19	21	23	23

(10 & less: very weak; 10 & above: weak; 15 & above good; 20 & above: very good)

Conclusions: A novel Schiff base ligand, the 3-amino-1,4-benzodioxine-2-carbaldehyde, and 3-aminopyridin-2-ol yielding the ligand 3-{(Z)-[(3-amino-1,4-benzodioxin -2-yl) methylidene] amino}pyridin-2-ol was synthesized through the condensation of 2-amino-4-oxo-4H-1-benzopyran-3-carbaldehyde with 2-amino-3-bromophenol. This ligand acts as a neutral, monodentate coordinating species via the nitrogen atom of the anilino group and the oxygen atom of the phenolic hydroxyl group. Its metal complexes with Mn (II), Co (II), Ni (II), Cu (II), Zn (II), Pd (II), and Pt (II) were successfully prepared and characterised using spectral techniques, magnetic susceptibility measurements, molar conductance, and elemental analysis. The data confirmed a 1:1 metal-to-ligand stoichiometry and indicated that all complexes are non-electrolytic in nature. Based on the analytical and spectroscopic findings, the complexes exhibit an octahedral geometry. Furthermore, antimicrobial assays revealed that the metal complexes possess enhanced antibacterial activity compared to the free Schiff base ligand.

Acknowledgement: The authors are thankful to the Principal and HOD, Department of Chemistry, Sathaye College, for providing the necessary Research Laboratory Facilities. University of Mumbai, HBSU Mumbai, for providing instrumental facilities.

Declaration of Competing Interest: The authors declare that they have no known competing financial interests or personal relationships that could have appeared to influence the work reported in this paper.

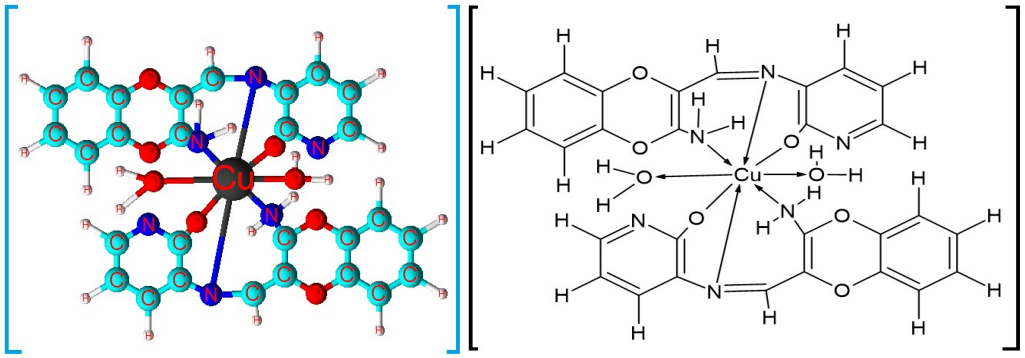

Figure -4: Structure of Complex

References:

1. Vigato PA, Tamburini S. The Challenge of Cyclic and Acyclic Schiff Bases and Related Derivatives. Coord Chem Rev. 2004; 248: 1717–2128. https://doi.org/10.1016/j.cct.2003.09.003
2. Patel NH, Parekh HM, Patel MN. Synthesis, characterisation and biological evaluation of manganese (II), cobalt (II), nickel (II), copper (II), and cadmium (II) complexes with mono-basic (NO) and neutral (NN) Schiff bases. Transit Met Chem. 2005; 30: 13–17. https://doi.org/10.1007/s11243-004-3226-5;

3. Ramesh R, Suganthy PK, Natarajan K. Synthesis, spectra and electrochemistry of Ru (III) complexes with tetradentate Schiff bases. Synth. React. Inorg Met-Org Chem. 1996; 26: 47–60. https://doi.org/10.1080/00945719608004245
4. Kaushik S, Paliwal SK, Iyer MR, Patil VM. Promising Schiff bases in antiviral drug design and discovery. Med Chem Res. 2023; 32: 1063−1076. https://doi.org/10.1007/s00044-023-03068-0.
5. Putaya AN, Ndahi NP, Bello HS, Mala G, Osunlaja AA, Garba H. Synthesis, characterisation and antimicrobial analysis of Schiff bases of o-phenylenediamine and 2-aminopyridine-3-carboxylic acid with ofloxacin and their metal (II) complexes. International Journal of Biological and Chemical Sciences. 2020; 14(1): 263-278. https://doi.org/10.4314/ijbcs.v14i1.22.
6. Choudhary MR, Lokhande MV. Some transitional metal ions complexes with 3-{[(e)-(4-fluorophenyl) methylidene] amino} benzoic acid and its microbial activity. Inter J Pharm Sci Res. 2014; 5(5): 1757-1766. https://doi.org/10.13040/IJPSR.0975-8232.5(5).1757-66.
7. Lokhande MV, Gulam FM. Spectral Studies of Some Transition Metal Ion Complexes with 4[(E)-(Ferrocene-1-Methylidene) Amino] Pyridin-2-ol. Journal of Applied Chemistry. 2014; 6(6): 36-42. https://doi.org/ 10.9790/5736-0663642.
8. George AA, Lokhande MV. Spectral Studies of New Organometallic Schiff Base Complexes and their Anti-Fungal Activity. Inter J Pharm Sci Res. 2017; 8(8): 3413-3420. https://doi.org/10.13040/IJPSR.0975-8232.8(8).3413-20.
9. Ibanphylla S, Kumar A, Kurbah KD, Lal RA. Synthesis, characterization and structure assessment of mononuclear and binuclear low-spin manganese(II) complexes derived from oxaloyldihydrazones, 1,10-phenanthroline and 2,2′-bipyridine. J Mol Struc. 1166; 2018:252-261. https://doi.org/10.1016/j.molstruc.2018.04.043
10. Kapade MG, Batawale PP, Raut UM, Lokhande MV. Synthesis, Characterisation of 2-[(Z)-{[6-Amino-2-(4-Chlorophenyl) Pyrimidin-4-Yl] Imino} Methyl]-4-Nitrophenol Schiff Base with Mn (II), Co (II), Ni (II), Cu(II), Zn (II), Pt (II) for their Nanoparticle and Antibacterial Studies. Rasayan J Chem. 2024; 17(4): 1426-1435. http://doi.org/10.31788/RJC.2024.1748925
11. Yusuf TL, Oladipo SD, Zamisa S, Kumalo HM, Lawal IA, Lawal MM, Mabuba N. Design of new Schiff-Base Copper (II) complexes: Synthesis, crystal structures, DFT study, and binding potency toward cytochrome P450 3A4. ACS Omega. 2021; 6: 13704–13718, https://doi.org/10.1021/acsomega.1c00906.
12. Kargar H, Ashfaq M, Fallah-Mehrjardi M, Behjatmanesh-Ardakani R, Munawar KS, Tahir, MN. Synthesis, crystal structure, spectral characterisation, theoretical and computational studies of Ni(II), Cu(II) and Zn(II) complexes incorporating Schiff base ligand derived from 4-(diethylamino) salicylaldehyde. Inorg Chim Acta. 2022;536: 120878 https://doi.org/10.1016/j.ica.2022.120878
13. Kapade MG, Batawale PP, Dalvi UM, Lokhande MV. Synthesis and Characterization of Novel Schiff Base Complexes of Mn(II), Co(II), Ni(II), Cu(II), Zn(II), Pd(II), Pt(II) Metal Ions for Microbial Activities and Their Nanoparticles. Inter J Pharml Sci Res. 2024;15(11): 3297-3306. https://doi.org/10.13040/IJPSR.0975-8232.15(11).3297-06.
14. Gulam FM, Lokhande MV. Electronic Spectra, Thermal Analysis, X-Ray Powder Diffraction, and SEM Studies of Organometallic Compound. Inter J Sci Res. 2013; 4(12): 457-460. https://doi.org/10.36106/IJSR.
15. Salehi M, Rahimifar F, Kubicki M, Asadi A. Structural, spectroscopic, electrochemical and antibacterial studies of some new nickel(II) Schiff base complexes. Inorga Chim Acta. 2016;443:28-35. https://doi.org/10.1016/j.ica.2015.12.016.
16. Emad Y, Ahmed M, Al-Sammarrae K, Salih N , Salimon J, Abdullah B. Metal complexes of Schiff base: Preparation, characterisation and antibacterial activity, Arab J Chem. 10(2); 2017: S1639-S1644. https://doi.org/10.1016/j.arabjc.2013.06.006

17. Sinicropi MS, Ceramella J, Iacopetta D, Catalano A, MariccondaCamillo RA, Saturnino C, El-Kashef H, Long P. Metal Complexes with Schiff Bases: Data Collection and Recent Studies on Biological Activities. Int J Mol Sci. 23(23); 2022:14840. https://doi.org/10.3390/ijms232314840
18. Manan MF, Kassim K, Manan MAFA. Synthesis, Characterisation and Conductivity Studies of Schiff Base Ligand Derived from Isatin and O-Phenylenediamine with its Cobalt(II) Metal Complex and Lithium-Schiff Base Compound. Malays J Anal Sci. 16(3); (2012): 318 – 324.
19. Ahmed AH , Moustafa MG. Spectroscopic, morphology and electrical conductivity studies on Co(II), Ni(II), Cu(II) and Mn(II)-oxaloyldihydrazone complexes. J Saudi Chem Soc. 24(5); 2020: 381-392.https://doi.org/10.1016/j.jscs.2020.02.003
20. Manimaran P, Balasubramaniyan S, Azam M, Rajadurai D, Al-Resayes SI, Mathubala G, Muthupandi MS, Tabassum Z, Khan I. Synthesis, Spectral Characterisation and Biological Activities of Co(II) and Ni(II) Mixed Ligand Complexes. Molecules. 2021; 26(4): 823. https://doi.org/10.3390/molecules26040823
21. Gulam FM, Lokhande MV. Some Transitional Metal Ion Complexes With 2,2'-{1,1'-Bi(Ferrocene-2,4-Dien-1-yl) -2,2'-Diylbis[Nitrilo(E) Methylylidene]} Bis (4-Chlorophenol) and Antimicrobial Activity. Journal of Applicable Chemistry.2013;2(6):1711-1720.
22. Paul T, Hossen F, Zahan KE, Haque M, Hossain S, Zamir R, Asraf A. Schiff base metal complexes: Synthesis, Characterisation, Thermal Analysis and Antibacterial Activity. Asian J Research Chem. 2020; 13(4):265-274. https://doi.org/10.5958/0974-4150.2020.00052.8.
23. Williams AF. Electronic Spectra and Magnetic Properties of Inorganic Compounds. In: A Theoretical Approach to Inorganic Chemistry. Springer, Berlin, Heidelberg. https://doi.org/10.1007/978-3-642-67117-3_4
24. Kargar H, Fallah-Mehrjardi M, Munawar KS. Metal complexes incorporating tridentate ONO pyridyl hydrazone Schiff base ligands: Crystal structure, characterisation and applications. Coord Chem Rev. 2024; 501:215587. https://doi.org/10.1016/j.ccr.2023.215587
25. Iacopetta D, Ceramella J, Catalano A, Mariconda A, Giuzio F, Saturnino C, Longo P, Sinicropi MS. Metal Complexes with Schiff Bases as Antimicrobials and Catalysts. Inorganics. 2023; 11(8): 320; https://doi.org/10.3390/inorganics11080320
26. Alorini T, Daoud I, Al-Hakimi AN, et al. An experimental and theoretical investigation of antimicrobial and anticancer properties of some new Schiff base complexes. Res Chem Intermed. 2023;49: 2023:1701–1730. https://doi.org/10.1007/s11164-022-04922-3
27. Ganesan TS, Elangovan N, Vanmathi V, Sowrirajan S, Chandrasekar S, Murthy KRS, Thomas R. Spectroscopic, Computational(DFT), Quantum mechanical studies and protein-ligand interaction of Schiff base 6,6-((1,2-phenylenebis (azaneylylidene)) bis (methaneylylidene)) bis(2-methoxyphenol) from o-phenylenediamine and 3- methoxy salicylaldehyde. J Ind Chem oc. 2022; 99: 100713 https://doi.org/10.016/j.jics.2022.100713
28. Shebl M. Mononuclear, homo- and hetero-binuclear complexes of 1-(5-(1-(2-aminophenylimino)ethyl)-2,4-dihydroxyphenyl) ethanone: synthesis, magnetic, spectral, antimicrobial, antioxidant, and antitumor studies. J Coord CheM. 2016; 69:199–214. https://doi.org/10.1080/00958972.2015.1116688
29. Hasan MM, Ahsan HM, Saha P, Naime J, Das AK, Asraf MA, Islam ABMN. Antioxidant, antibacterial and electrochemical activity of (E)-N-(4 (dimethylamino) benzylidene)-4H-1,2,4-triazol-4-amine ligand and its transition metal complexes. Results Chem. 2021; 3: 100115 https://doi.org/10.1016/j.rechem.2021.100115
30. El-ghamry MA, Elzawawi FM, Aziz AAA, Nassir KM, Abu-El-Wafa SM. New Schiff base ligand and its novel Cr(III), Mn(II), Co(II), Ni(II), Cu(II), Zn(II) complexes: spectral investigation, biological applications, and semiconducting properties. Sci Rep. 2022; 12: 17942, https://doi.org/10.1038/s41598-022-22713-z